Length Regulation of Active Biopolymers by Molecular Motors

Denis Johann, Christoph Erlenkämper, and Karsten Kruse
Theoretische Physik, Universität des Saarlandes, 66041 Saarbrücken, Germany
(Received 5 March 2012; published 22 June 2012)

For biopolymers like cytoskeletal actin filaments and microtubules, assembly and disassembly are inherently dissipative processes. Molecular motors can affect the rates of subunit removal at filament ends. We introduce a driven lattice-gas model to study the effects of motor-induced depolymerization on the length of active biopolymers and find that increasing motor activity sharpens unimodal steady-state length distributions. Furthermore, for sufficiently fast moving motors, the relative width of the length distribution is determined only by the attachment rate of motors. Our results show how established molecular processes can be used to robustly regulate the size of cytoskeletal structures like mitotic spindles.

DOI: 10.1103/PhysRevLett.108.258103 PACS numbers: 87.16.Ka, 05.40.−a, 87.10.Hk, 87.16.Nn

Cytoskeletal filaments, notably F-actin and microtubules, take an important part in determining the mechanical properties and internal organization of cells [1]. These biopolymers are considered to be ''active'' as their assembly depends on the hydrolysis of nucleotide triphosphates, which can generate interesting nonequilibrium behavior. For example, length changes in response to variations in the microenvironment are faster for active filaments than for equilibrium polymers [2]. Furthermore, cytoskeletal filaments can treadmill such that subunits are on average added at one end and removed from the other [3–5]. This phenomenon relies on structural differences between the two ends, which are referred to as the ''plus'' and the ''minus'' end, respectively. In striking contrast to passive polymers, treadmilling filaments can display unimodal length distributions [6]. This might be physiologically relevant for muscle sarcomeres [7] or mitotic spindles [8], where filament lengths are tightly regulated.

Microtubule length regulation in mitotic spindles notably involves molecular motors of the kinesin superfamily [1]. These enzymes can convert chemical energy into directed motion along microtubules. At the same time, some kinesin motors induce the removal of tubulin subunits at microtubule ends [9,10]. In this way, effectively length-dependent depolymerization rates can be generated [11–14], which regulate the length of individual microtubules.

In addition to their biological relevance, molecular motors have become a paradigm for studying transport phenomena. They have notably motivated the study of one-dimensional lattice models like the Totally Asymmetric Simple Exclusion Process (TASEP) [15–18] and revealed a number of genuine nonequilibrium phenomena. In the TASEP, particles enter the lattice at one end. Unless hindered by steric interactions with other particles they hop towards the opposing end, where they eventually leave the lattice. In this model, boundary-induced phase transitions have been found [19]. If motors can enter and leave the system anywhere along the lattice, pinned domain walls can emerge [20].

Few works have so far considered the interplay between the nonequilibrium dynamics of motors and filaments. It was shown that motors transporting filament nucleators are capable of organizing an ensemble of active filaments into asters and waves [21–23] and of polarizing a dynamic filament network [24,25]. Furthermore, treadmilling stabilizes contractile bundles of filaments and motors [26] and dynamic filaments typically prevent the formation of motor jams [27,28].

Motivated by minus-end directed kinesins, we study in this work the effects of molecular motors on the length distribution of treadmilling filaments. *In vitro* experiments showed that the motor Kar3p increases the depolymerization rate at the minus ends of treadmilling microtubules [29,30]. The motor KLP10A is involved in spindle-length regulation in the fruit fly *Drosophila melanogaster*. Observations of spindles *in vivo* strongly suggest that also this motor increases subunit removal at microtubule minus ends [31]. Using a one-dimensional driven lattice gas, we find that increased motor hopping typically sharpens unimodal length distributions. Remarkably, for motors moving sufficiently fast the length distribution is completely determined by the motor attachment rate.

Consider a dynamic lattice, where individual sites represent subunits of the filament; see Fig. 1(a). The plus end is located at site $i = 1$, while the minus end is at $i = L$. Molecular motors are represented by point particles on the lattice. As in the TASEP, a particle on site i can hop at rate γ to site $i + 1$ provided that the latter is empty. In addition, motors attach to empty sites at rate ω and detach from occupied sites at rate $\bar{\omega}$. Empty sites are added to the plus end at rate α. Occupied sites are removed together with the bound motor from the minus end at rate β. The case of subunit removal from the plus end is discussed in the companion Letter, Ref. [32]. For $L = 1$ the only remaining site cannot be removed. In the following, we rescale all rates by α. If β is below a critical value β_c, the filament

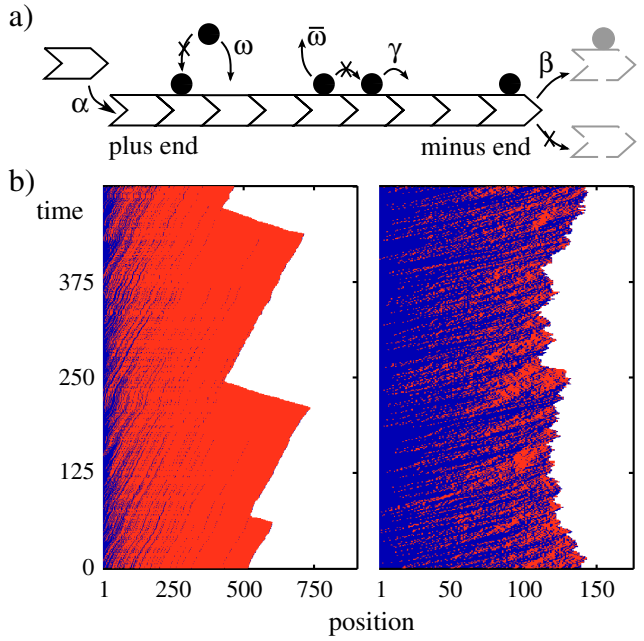

FIG. 1 (color online). Motor-induced shortening of an active biopolymer. (a) Illustration of the model: Empty sites are added at the plus end at rate α and occupied sites are removed from the lattice at the minus end at rate β. Particles bind to empty sites at rate ω and hop at rate γ to empty sites towards the minus end. In the following, all rates are scaled by α. (b) Examples of the steady-state dynamics with $\beta = 10$, $\omega = 0.01$, and $\gamma = 0$ (left) and $\gamma = 2$ (right). Empty sites are shown in blue, occupied sites in red.

length will diverge. We will limit ourselves to the case $\bar{\omega} = 0$, such that $\beta_c = 1$ independently of γ and ω and consider only $\beta > 1$. For $\bar{\omega} > 0$, β_c can diverge, in which case no steady state exists. As long as $\beta > \beta_c$, though, the system behavior does not depend qualitatively on $\bar{\omega}$.

Stochastic simulations show that the system length fluctuates around a well-defined mean value, see Fig. 1(b). The corresponding length distributions are unimodal with decreasing average length and width for increasing hopping rate γ; see Fig. 2(a).

Qualitatively, this behavior can be easily understood: We start by noting that the average probability for a site to be occupied increases monotonically with its distance to the plus end; see Fig. 2(b). This is because new sites that are added at the plus end are initially empty. Consequently, the probability of having an occupied site at the minus end and thus the effective detachment rate increase with the system length. Since the probability of finding an occupied site approaches 1 as its distance to the plus end increases, there must be a critical length below which the system tends to grow, while otherwise it shrinks on average. With increasing values of γ the time during which the minus end is empty decreases and fluctuations in the rate of subunit removal are reduced; see Fig. 1(b). This leads to smaller averages and sharper length distributions.

To study the quality of motor-induced length regulation, we present in Fig. 3 the relative width $Q = \sigma/\langle L \rangle$, where $\langle L \rangle$ is the average length and $\sigma^2 = \langle L^2 \rangle - \langle L \rangle^2$ the corresponding variance, as a function of β and γ. Except for a tiny region at $\beta \gtrsim 1$, the value of Q decreases with increasing γ. An increased motor activity will thus typically lead to a better defined length distribution. Note, however, that for $\gamma \gtrsim 1$, the value of Q quickly approaches 0.1. As we will show below, in general, the saturation value is $Q = \sqrt{\omega(1+\omega)}$.

We will now discuss the length distribution in more detail. To this end, we first analyze the motor distribution for a semi-infinite filament ($\beta = 0$). Let $n_i(t) = 0,1$ be the occupation number of site i at time t and consider the average occupation number $0 \leq \rho_i \equiv \langle n_i \rangle \leq 1$. As the value of γ is increased, the profile develops a region of increasing steepness which in the limit $\gamma \to \infty$ turns into a "shock" separating a domain of empty sites from a domain of occupied sites [20,27,33].

To calculate the average occupation number of site i in steady state, we use a mean-field approximation,

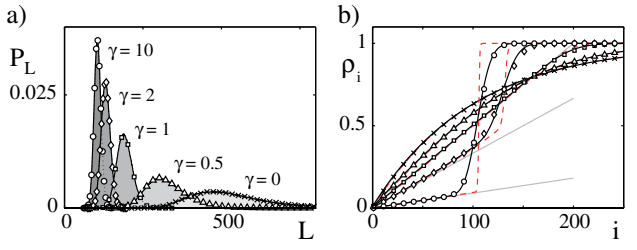

FIG. 2 (color online). Effects of the motor hopping rate γ on the length distribution. (a) Steady-state length distributions for various values of γ, $\beta = 10$, and $\omega = 0.01$. (b) Average occupation probability of lattice sites. Symbols as in (a). Red dashed lines represent the solution of Eq. (1), while full black lines are given by Eq. (2). Gray lines indicate the slope $\omega/(1+\gamma)$ at $i = 1$; see text. Values are shown for every tenth data point.

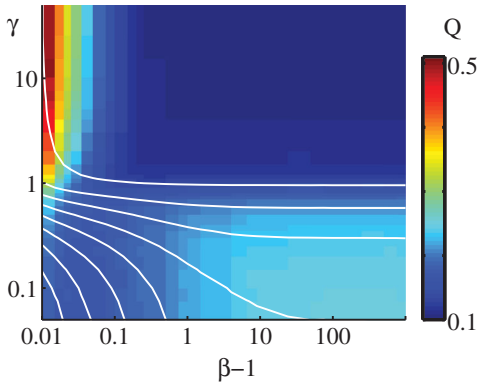

FIG. 3 (color). Relative width Q of the length distribution as a function of the motor hopping rate γ and the removal rate β for $\omega = 0.01$. White lines connect loci of equal average length.

$\langle n_i n_{i+1}\rangle = \rho_i \rho_{i+1}$, such that the time evolution of the mean-field density ρ_i^{mf} is given by

$$\dot{\rho}_i^{\mathrm{mf}} = \omega(1-\rho_i^{\mathrm{mf}}) + \gamma\rho_{i-1}^{\mathrm{mf}}(1-\rho_i^{\mathrm{mf}}) - \gamma\rho_i^{\mathrm{mf}}(1-\rho_{i+1}^{\mathrm{mf}}) + \rho_{i-1}^{\mathrm{mf}} - \rho_i^{\mathrm{mf}} \quad (1)$$

for $i > 1$ with boundary condition $\dot{\rho}_1^{\mathrm{mf}} = \omega(1-\rho_1^{\mathrm{mf}}) - \gamma\rho_1^{\mathrm{mf}}(1-\rho_2^{\mathrm{mf}}) - \rho_1^{\mathrm{mf}}$. The terms on the right-hand side account for attachment of motors to empty sites, particle hopping and addition of sites to the plus end, respectively. In steady state, ρ_i^{mf} can be obtained recursively for $i > 1$ with ρ_1^{mf} being determined by the flux-balance condition $\omega\sum_{i=1}^{\infty}(1-\rho_i^{\mathrm{mf}}) = 1$. This condition reflects that, in steady state, the total rate of motor attachment must equal the rate of site addition at the plus end.

The above approach neglects correlations in addition to those between the occupation numbers of neighboring sites. This is because the time T having passed since site i has been incorporated into the system is a stochastic variable. Similar to the TASEP, the former are negligible [17,18], while the latter give an important contribution. The probability distribution of times T is given by $p_i(T) = T^{i-1}e^{-T}/(i-1)!$, because $i-1$ new sites were added at rate 1 since site i has joined the lattice. Assuming that the occupation probability of site i at age T is ρ_T^{mf}, we then get

$$\rho_i = \sum_{j=1}^{\infty} \rho_j^{\mathrm{mf}} p_i(j). \quad (2)$$

The motor profile obtained in this way is in very good agreement with the simulation results; see Fig. 2(b).

Below we make use of a continuum approximation $\rho(x)$ for the motor density, where we use $\rho_{i\pm1} \simeq \rho(x) \pm d\rho(x)/dx$. For $\gamma < 1$, the solution of the corresponding steady-state equations with $\rho(0) = 0$ is given by $\omega x = 2\gamma\rho + (\gamma-1)\ln(1-\rho)$. For $\gamma > 1$ this continuum solution has a discontinuity at the shock position x_s and the density is well described by the linear profile $\rho_{\mathrm{lin}}(x) = \omega x/(1+\gamma)$ if $x < x_s$ and $\rho = 1$ if $x > x_s$. x_s is determined by the flux-balance condition, which now reads $\omega\int_0^{x_s}(1-\rho_{\mathrm{lin}}(x))dx = 1$.

We will now turn to the system's length distribution P_L in steady state. We can write the time evolution in the form

$$\dot{P}_L = j_L - j_{L+1}, \quad (3)$$

where j_{L+1} is the probability current from a state of length L to a state of length $L+1$, together with the boundary condition $j_1 = 0$. In steady state, $\dot{P}_L = 0$ and we have $j_L = 0$ for all $L = 1, 2, \ldots$ The contribution to the current j_L due to the addition of subunits at the plus end is P_L. Accounting for subunit removal at the minus end is much more involved as it depends on the motor distribution in the system. In the following, we propose an approximate expression for the current j_L.

To calculate the rate at which the site at the minus end is removed from the system, we will again neglect correlations between neighboring sites, but retain the stochasticity of the sites' ages. Consider a system of length L and let ℓ be the length at which the current last site had reached the minus end. Furthermore, the time τ indicates the time span that has passed since this event. The probability that site L is empty will be denoted by $p_0(L,\ell,\tau)$, while $p_1(L,\ell,\tau)$ denotes the probability that it is occupied. Finally, $p_x(L,\ell,\tau)$ is the probability that this site was removed prior to the time τ. We have $p_0 + p_1 + p_x = 1$. If p_x is known, then $\partial_\tau p_x$ is the rate at which the site is removed at time τ after it has become the minus end. For a system of length L, the average removal rate of subunits that have become the minus end as the system had length ℓ is then

$$\beta_{\ell,L} = \int d\tau \frac{\tau^{L-\ell}}{(L-\ell)!} e^{-\tau}\partial_\tau p_x(L,\ell,\tau). \quad (4)$$

The sum over all these rates weighted by the probability that the system has length ℓ finally gives the contribution of removal events to the probability current. Consequently, the steady-state condition reads

$$j_L = P_L - \sum_{\ell=1}^{L+1} \beta_{\ell,L+1} P_\ell = 0. \quad (5)$$

It remains to determine $\partial_\tau p_x = -\partial_\tau(p_0 + p_1)$. The probabilities $p_0(L,\ell,\tau)$ and $p_1(L,\ell,\tau)$ evolve according to

$$\frac{\partial}{\partial\tau}\begin{pmatrix} p_0 \\ p_1 \end{pmatrix} = \begin{pmatrix} -\omega - \gamma\rho_{\ell-1+\tau} & 0 \\ \omega + \gamma\rho_{\ell-1+\tau} & -\beta \end{pmatrix}\begin{pmatrix} p_0 \\ p_1 \end{pmatrix}. \quad (6)$$

This equation accounts for the occupation of sites by motor attachment and motor hopping as well as removal of occupied sites, but neglects correlations between the last and the second but last site. We choose as initial conditions $p_0(L,\ell,\tau=0) = 1-\rho_\ell$ and $p_1(L,\ell,\tau=0) = \rho_\ell$. Eqs. (3)–(6) specify a nonlocal, but Markovian jump process for the system length.

The steady-state solution of this jump process can be given analytically, however, the expressions are cumbersome and not very revealing. In Fig. 4 we plot the resulting average length $\langle L\rangle$ and standard deviation σ as a function of β for various values of γ and ω. In these calculations, we have used the motor distribution obtained in the continuum limit. For $\gamma = 0$ the solution of the jump process is identical to the simulation results. In contrast to the motor distribution discussed above, for $\gamma > 0$, correlations between adjacent sites now become important and lead to increasing deviations from the numerical results as γ/ω increases.

We can gain complementary insights for large hopping rates γ by analyzing the limit $\gamma \to \infty$. In this limit, the length dynamics is described by a two-dimensional random walk. Indeed, the system is in this case divided into an empty region I of length M starting at the plus end and a fully occupied region II of length $N = L - M$ extending to the minus end. The probability $P_{M,N}$ evolves according to

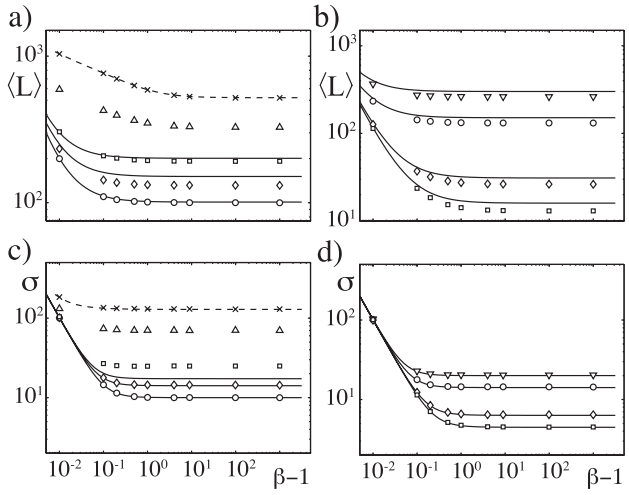

FIG. 4. Mean length and variance of length distribution as a function of the removal rate β for different values of the hopping rate γ (a),(c) and of the motor attachment rate ω (b),(d). Symbols represent simulation results, full lines are given by Eqs. (8) and (9) for $\langle L\rangle$ and σ, respectively. Dashed lines are obtained from solutions of the jump process defined by Eqs. (4)–(6). In (a),(c) $\omega = 0.01$ and $\gamma = 0$ (×), 0.5 (△), 1 (□), 2 (◇), 10^5 (○); in (b),(d) $\gamma = 2$ and $\omega = 0.005$ (▽), 0.01 (○), 0.05 (◇), 0.1 (□).

$$\dot{P}_{M,N} = P_{M-1,N} - P_{M,N} + \beta(P_{M,N+1} - P_{M,N}) + \omega((M+1)P_{M+1,N-1} - MP_{M,N})) \tag{7}$$

for M, $N > 1$. The system is complemented by no-flux boundary conditions for M, $N = 1$.

We now consider the marginal distributions for M and N separately. The steady-state equation for the distribution of M, $P_M^{\mathrm{I}} = \sum_{N=1}^{\infty} P_{M,N}$, only depends on P_M^{I}. Its solution is given by $P_M^I = \frac{\omega^{-M}}{M!}\exp(-\frac{1}{\omega})$. To calculate the steady-state distribution of N, we make a mean-field assumption and write $\sum_{M=0}^{\infty} MP_{M,N} = \langle M\rangle P_N^{\mathrm{II}}$, which gives $P_N^{\mathrm{II}} = (\beta-1)\beta^{-N+1}$. Consequently, we obtain $\langle L\rangle_\infty = \langle M\rangle + \langle N\rangle = \omega^{-1} + (\beta-1)^{-1}$ and $\sigma_\infty^2 = \omega^{-1} + \beta^2(\beta-1)^{-2}$. Comparison of $\langle L\rangle_\infty$ and σ_∞ with numerical data shows good agreement; see Fig. 4. In the limit $\beta \to \infty$ they yield $Q = \sqrt{\omega(1+\omega)}$ as announced above.

These considerations can be extended to values of $\gamma < \infty$ by assuming that there is still a fully occupied domain, while the second domain is now partially filled. The shock position x_s still describes a random walk with an effective hopping rate to the left that is given by the quotient of the motor current to the site $i = M$, $\gamma\rho(M-1)(1-\rho(M))$, and the shock height $1-\rho(M)$ [33,34]. We approximate the motor distribution in the partially occupied domain by a linear profile and use ρ_{lin}. Again, we make a mean-field assumption and consider the two domains to be independent of each other. In first order in γ^{-1} we then get

$$\langle L\rangle_\gamma = \langle L\rangle_\infty + \frac{1}{\gamma\omega}, \tag{8}$$

$$\sigma_\gamma^2 = \sigma_\infty^2 + \frac{2}{\gamma\omega}. \tag{9}$$

As we have seen above correlations for $\gamma \neq 0$ are in general important. We estimate the correction to the variance due to correlations to be of the same order as the correction to the variance if both processes were uncorrelated. This explains the factor 2 in the correction term to σ^2. The agreement is satisfying for $\gamma > 1$; see Fig. 4.

In conclusion, we have shown that the activity of molecular motors can sharpen the length distribution of treadmilling filaments. Furthermore, we have found that the presence of motors makes the filament length distribution robust against variations in system parameters as long as the motors are faster than the average filament growth velocity. In this regime the filament length essentially depends only on the motor attachment rate. A quantitative model of motor-induced microtubule length regulation should take into account several additional features: the state of the nucleotides bound to tubulin subunits, addition of subunits at the minus- and removal at the plus end, and the presence of several protofilaments in a microtubule. We expect, however, that our findings will *cum grano salis* be unaffected by these changes.

We thank E. Frey and A. Melbinger for sharing their unpublished work with us and them as well as L. Santen for helpful discussions. This work was in part supported by the Deutsche Forschungsgemeinschaft through the Research Training Group GRK 1276.

[1] D. Bray, *Cell Movements: From Molecules to Motility* (Garland, New York, 2001), 2nd ed.
[2] D. Swanson and N. S. Wingreen, Phys. Rev. Lett. **107**, 218103 (2011).
[3] A. Wegner, J. Mol. Biol. **108**, 139 (1976).
[4] T. D. Pollard, J. Cell Biol. **103**, 2747 (1986).
[5] V. I. Rodionov and G. G. Borisy, Science **275**, 215 (1997).
[6] C. Erlenkämper and K. Kruse, Phys. Biol. **6**, 046016 (2009).
[7] R. Littlefield and V. M. Fowler, Annu. Rev. Cell Dev. Biol. **14**, 487 (1998).
[8] J. Gaetz and T. M. Kapoor, J. Cell Biol. **166**, 465 (2004).
[9] L. Wordeman, Curr. Opin. Cell Biol. **17**, 82 (2005).
[10] J. Howard and A. A. Hyman, Curr. Opin. Cell Biol. **19**, 31 (2007).
[11] V. Varga, J. Helenius, K. Tanaka, A. A. Hyman, T. U. Tanaka, and J. Howard, Nat. Cell Biol. **8**, 957 (2006).
[12] V. Varga, C. Leduc, V. Bormuth, S. Diez, and J. Howard, Cell **138**, 1174 (2009).
[13] L. E. Hough, A. Schwabe, M. A. Glaser, J. R. McIntosh, and M. D. Betterton, Biophys. J. **96**, 3050 (2009).
[14] L. Reese, A. Melbinger, and E. Frey, Biophys. J. **101**, 2190 (2011).

[15] J. T. MacDonald, J. H. Gibbs, and A. C. Pipkin, Biopolymers **6**, 1 (1968).
[16] B. Derrida, E. Domany, and D. Mukamel, J. Stat. Phys. **69**, 667 (1992).
[17] G. Schütz and E. Domany, J. Stat. Phys. **72**, 277 (1993).
[18] B. Derrida, M. R. Evans, V. Hakim, and V. Pasquier, J. Phys. A **26**, 1493 (1993).
[19] J. Krug, Phys. Rev. Lett. **67**, 1882 (1991).
[20] A. Parmeggiani, T. Franosch, and E. Frey, Phys. Rev. Lett. **90**, 086601 (2003).
[21] E. N. Cytrynbaum, V. Rodionov, and A. Mogilner, J. Cell Sci. **117**, 1381 (2004).
[22] K. Doubrovinski and K. Kruse, Phys. Rev. Lett. **99**, 228104 (2007).
[23] K. Doubrovinski and K. Kruse, Eur. Phys. J. E **31**, 95 (2010).
[24] R. J. Hawkins, O. Bénichou, M. Piel, and R. Voituriez, Phys. Rev. E **80**, 040903 (2009).
[25] P. Greulich and L. Santen, Phys. Rev. E **84**, 060902 (2011).
[26] P. Guthardt Torres, K. Doubrovinski, and K. Kruse, Europhys. Lett. **91**, 68 003 (2010).
[27] K. E. P. Sugden and M. R. Evans, J. Stat. Mech. (2007) P11013.
[28] M. Ebbinghaus, C. Appert-Rolland, and L. Santen, Phys. Rev. E **82**, 040901(R) (2010).
[29] S. A. Endow, S. J. Kang, L. L. Satterwhite, M. D. Rose, V. P. Skeen, and E. D. Salmon, EMBO J. **13**, 2708 (1994).
[30] S. A. Endow, Eur. J. Biochem. **262**, 12 (1999).
[31] G. C. Rogers, S. L. Rogers, T. A. Schwimmer, S. C. Ems-McClung, C. E. Walczak, R. D. Vale, J. M. Scholey, and D. J. Sharp, Nature (London) **427**, 364 (2004).
[32] A. Melbinger, following Letter, Phys. Rev. Lett. **108**, 258104 (2012).
[33] M. R. Evans, R. Juhász, and L. Santen, Phys. Rev. E **68**, 026117 (2003).
[34] A. Kolomeisky, G. M. Schütz, E. B. Kolomeisky, and J. P. Straley, J. Phys. A **31**, 6911 (1998).